AN IN-ORBIT DEMONSTRATION OF RECOVERY FROM FLAT SPIN FOR A MOMENTUM BIAS CONTROLLED COMMUNICATIONS SPACECRAFT: OTS

C K Leong & N Matthews

British Aerospace
Space and Communications Division
Stevenage, UK.

L V Holtz & A G Bird

European Space Research and
Technology Centre (ESTEC)
Noordwijk, The Netherlands.

ABSTRACT

A straightforward attitude recovery technique for momentum biased satellites is presented. It applies to those anomalies in which no significant external torques act on the satellite and hence the total angular momentum vector is conserved. The technique is based on a control law which minimizes the spin energy of the satellite body using the momentum wheel as the only actuator. It requires only reasonably accurate estimates of spacecraft inertias, which can be determined in orbit by a method described in the paper. By the inclusion of a first order predictor the control loop is shown to cope with significant delays in data acquisition and control implementation. The recovery technique is therefore suitable for implementation on-board or under ground control. An experiment has successfully demonstrated its effectiveness with ESA's communications satellite OTS.

Keywords: Arbitrary Spin Recovery, Core Energy Minimization, Spin Equilibrium Points, Flat Spin Manoeuvre, Momentum Bias Spacecraft, OTS Flat Spin Test.

1. INTRODUCTION

For a momentum biased spacecraft where attitude is stabilised using a single fixed momentum wheel or a skewed wheel system, large nutation or flat spin results when the momentum wheel is allowed to run down. Recovery using on-board control has been studied in the past by the European Space Agency which led to the adoption of a robust failsafe sun-pointing technique capable of handling all conceivable contingencies including the case described above. This technique, however, requires Sun-Spacecraft-Earth orthogonality for resumption of normal attitude from Sun pointing mode, which may involve a long service outage of up to half a day.

The new generation of communications satellites has a more stringent requirement for recovery within a few hours and furthermore there is a desire to extend this requirement to satellites already in orbit. Although various algorithms and techniques (Ref. 1-3) for recovery from arbitrary spin are well known, the need for additional on-board mechanical hardware, sensitivity to modelling errors such as uncertainty in the values of the inertias, and the problem of telemetry data acquisition and accurate wheel speed control for implementation under ground control have presented challenges towards the production of a realistic recovery procedure.

This paper presents a simple technique for recovery from arbitrary spin which has overcome these difficulties. For loss of nominal spacecraft attitudes not involving significant external torques, it is feasible to achieve recovery using this technique within one hour. The heart of the recovery technique is an angular momentum control loop which leads to minimization of the spacecraft spin energy and thus reduces nutation. A model of rigid body spacecraft motion, based upon the dynamic equations of angular momentum, may be used to optimise the control loop. By implementing the spacecraft model and control algorithm in a desktop computer, various procedures for recoveries or configuration stabilization from any nutation and flat spin configurations have been analysed. Finally an experiment on OTS is described, which demonstrated the effectiveness of the recovery procedure under ground control.

2. ANALYSIS

The spacecraft treated in this study is shown in Fig. 1. For the benefit of adopting the same notation as in the later section which describes the flat spin recovery experiment on OTS, the following nominal spacecraft configuration is assumed without loss of generality: the orthogonal body axes x, y and z are coincident with the principal inertia axes; in nominal on-station attitudes the x axis of the spacecraft (the roll axis) points in the direction of motion of the spacecraft, the y axis (pitch axis) is parallel to the Earth's rotational axis and points southwards, and the z axis (yaw axis) points towards the Earth. Furthermore, the principal inertias of the spacecraft are I_{xx}, I_{yy} and I_{zz} with $I_{zz} > I_{xx} > I_{yy}$. The inertia cross products I_{xy}, I_{xz} and I_{yz} are relatively small and may be neglected. The nominal orientation of the spacecraft is maintained by the inclusion of a single or set of momentum wheel(s) whose total angular momentum vector is aligned parallel to or coincident with the minimum inertia axis, i.e. the y axis.

Proceedings of the Second International Symposium on Spacecraft Flight Dynamics, Darmstadt, FR Germany, 20–23 October 1986 (ESA SP-255, Dec. 1986)

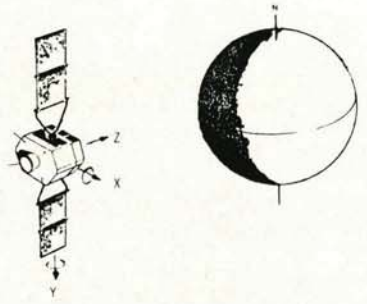

Fig. 1 Nominal spacecraft configuration

The rigid body rotational motion of the spacecraft may be described by Eqs. 1-3, where (H_{xs}, H_{ys}, H_{zs}) are the components of spacecraft body angular momentum (with the momentum wheel(s) locked)

$$\dot{H}_{xs} = (H_{ys} + H_r)\, H_{zs}/I_{zz} - H_{zs}H_{ys}/I_{yy} \qquad (1)$$

$$\dot{H}_{ys} = H_{zs}\, H_{xs}/I_{xx} - H_{xs}\, H_{zs}/I_{zz} - \dot{H}_r \qquad (2)$$

$$\dot{H}_{zs} = H_{xs}\, H_{ys}/I_{yy} - (H_{ys} + H_r)\, H_{xs}/I_{xx} \qquad (3)$$

and H_r is the total angular momentum of the wheel(s). To simplify the discussion, we shall now assume the case of a single y axis momentum wheel whose spin axis inertia is I_r. Furthermore the term 'angular momentum' is simply referred to as 'momentum'. Fig. 2 shows the orientation of these parameters as defined in Eqs. 1-3.

In considering arbitrary spin motion of a spacecraft it is convenient to regard the total spacecraft body momentum vector H in the spacecraft body frame, where $H^2 = H_{xs}^2 + H_{ys}^2 + H_{zs}^2$. Referring to Fig. 2 the orientation of H relative to the y and z axes are described by the nutation angle θ and phase angle ϕ respectively. After Ref. 1 we may define the 'spacecraft core energy' as 'total spacecraft spin energy less the spin energy due to the motion of the wheel relative to the spacecraft body'. The motion of the spacecraft body is dependent on certain equilibrium positions of H and the level of the spacecraft core energy. Ref. 1 gives these equilibrium positions as :

$$\theta = 0° \text{ or } 180°, \text{ for all } \gamma \text{ values} \qquad (4)$$

$$\phi = 0° \text{ or } 180° \text{ and } \theta = \cos^{-1}[\gamma/(1-I_{yy}/I_{zz})]$$

$$\text{for } |\gamma/(1 - I_{yy}/I_{zz})| < 1 \qquad (5)$$

$$\phi = 90° \text{ or } -90° \text{ and } \theta = \cos^{-1}[\gamma/(1-I_{yy}/I_{xx})]$$

$$\text{for } |\gamma / (1-I_{yy}/I_{xx})| < 1 \qquad (6)$$

where the normalised wheel momentum, $\gamma = H_r/H$.

The first physical implication of Eqs. 4-6 is the well known fact that if the wheel momentum H_r is above a certain critical value then there are only two equilibrium positions for H (i.e. θ = 0° or 180°). Ref. 1 has shown that only one of them is stable, that is the one which corresponds to H being in the same direction as H_r. Furthermore, H is in this stable orientation only if the spacecraft core energy is at a minimum. Under normal operating conditions this is achieved only through natural energy dissipating mechanisms such as fuel slosh and flexure of appendages. If the wheel momentum H_r is below the critical value, there is an additional set of two or four equilibrium positions depending on whether one or both of Eqs. 5-6 are satisfied. For spacecraft with $I_{zz} > I_{xx} > I_{yy}$, this critical value is given by $H_{rc} = H(1-I_{yy}/I_{zz})$.

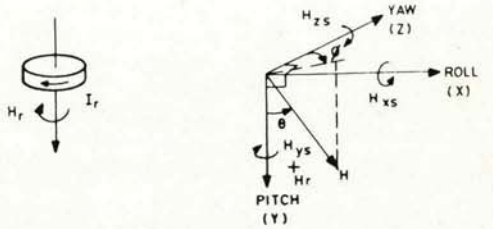

Fig. 2 Spacecraft angular momentum coordinate system

With the wheel momentum below H_{rc}, it is found that only the pair of equilibria located in the y-z plane corresponding to ϕ = 0° or 180°, are stable. In a two dimensional (H_{xs}, H_{zs}) momentum space these stable equilibrium positions projected onto the H_{zs} axis are given by $\pm H \sin\theta_z$, where $\theta_z = \theta$ defined in Eq. 5. As illustrated in Fig. 3 the other additional pair of equilibria is located at $\pm H \sin\theta_x$ on the H_{xs} axis, where $\theta_x = \theta$ defined in Eq. 6. The spin motion of the spacecraft at sub critical wheel speeds may be usefully illustrated by the movement of the total momentum vector H, projected onto this body fixed two dimensional momentum space. It must be emphasised that in practice H is stationary in inertial space in the absence of any external torque acting on the spacecraft, and it is the distribution of H along the three orthogonal principal axes which variesas the spacecraft spins or tumbles 'arbitrarily'.

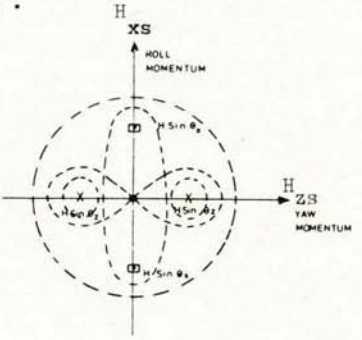

Fig. 3 Spin equilibrium and projected paths of H in 2-D momentum space

Depending upon the level of the spacecraft core energy, the projection of H traces different closed paths enclosing some or all of the existing equilibrium positions. For low spacecraft core energies, these paths tend to centre on one of the stable positions on the H_{zs} axis. The lower the spacecraft core energy the tighter the closed path will be to one of the stable positions. When the core energy is minimum, it is in the y-z plane with H_{xs} zero. In the limit when the wheel momentum is zero the stable equilibria correspond to H being parallel to the H_{zs} and this is generally

known as the final flat spin configuration.

In general, the recovery of spacecraft attitude from an arbitrary spinning or tumbling state means simply the control of the orientation of the total momentum vector H in the momentum space such that H_{xs} and H_{zs} are finally zero. This configuration corresponds to minimum spacecraft core energy, it follows that any recovery procedure which begins from sub critical wheel speed conditions should involve minimization of this energy as the momentum wheel is spun up. In particular when the wheel speed is approaching the critical value, the projected H should be as close to the H_{zs} axis as possible, in order to ensure that the H_{xs} and H_{zs} values are acceptably small after the wheel speed has increased beyond the critical value and the residual nutation is thus small.

One technique which may be used to meet the above requirements is based on the setting up of an H_{xs} deadband, ± m, and a H_{xs} control algorithm to actively reduce the value of H_{xs} whenever it is outside ± m. It is then a simple matter of spinning up the momentum wheel at an acceptable nominal rate and enabling the H_{xs} control loop when the wheel speed is approaching the critical value. The timing of imposing H_{xs} control is primarily dependent on the rate of wheel spin up and the effectiveness of the H_{xs} control loop. Fig. 4 shows a simple H_{xs} control law which is derived from Eq. 1. Depending on the value of H_{xs}, the signs of H_{xs} and H_{zs}, and the state of wheel momentum H_r in relation to the parameter $C = H_{ys}(I_{zz}/I_{yy} - 1)$, the control law demands the appropriate wheel torque level T^0, T^- or T^+. For recovery from sub critical wheel speed conditions, T^0 is set to increase the wheel momentum, at a nominal rate, T^- to reduce the wheel momentum, and T^+ to increase the wheel momentum at a higher than nominal rate.

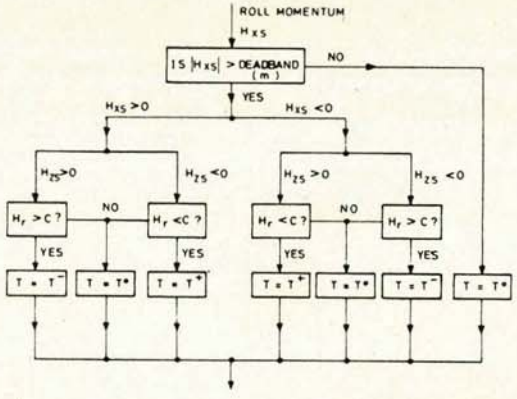

Fig. 4 Schematic of H_{xs} control loop algorithm

The recovery is first initiated by wheel torque $T = T^0$. When the H_{xs} control loop is activated the desired wheel torque may change to T^+ or T^- if H_{xs} is outside the defined deadband ± m, and then revert to T^0 once H_{xs} has been reduced to within ± m. In order to apply such a control law to a spacecraft already in orbit, and whose on-board control algorithms cannot be changed, it is necessary to implement the law in the spacecraft control station on the ground. Unfortunately, this brings about lengthy delays in the loop due to ground processing time and operator reaction time. For this reason a first order predictor for H_{xs} has to be used. This involves replacing H_{xs} by $[H_{xs} + K(\dot{H}_{xs})]$ in the comparison with deadband ± m where K is a constant depending on the delay and $\dot{H}_{xs}$ is an estimate of the rate of change of H_{xs}. The latter may be based on the difference between two consecutive measurements of H_{xs}. It is interesting to note that in cases where the implementation delay is approaching half a period of the projected H path, it is necessary to reverse the H_{zs} sign logic in Fig. 4 in order to preserve the correct phasing between spacecraft spin dynamics and control implementation.

For the H_{xs} control loop to function correctly it is necessary to obtain a reasonably accurate estimate of the spacecraft inertias. Recall that for sub critical wheel speeds the stable equilibrium points of H projected in a two dimensional (H_{xs}, H_{zs}) momentum space are given by $H\sin\theta_z$. These points are linked to the spacecraft inertias I_{yy} and I_{zz} by Eq. 5 or more explicitly in the form of Eq. 7 where $I_{cb} = (1 - I_{yy}/I_{zz})$; $\omega_{ze} = H\sin\theta_z/I_{zz}$ is the stable equilibrium yaw (z-axis) rate corresponding to a sub critical wheel speed Ω_r, and Ω_n is the nominal wheel speed.

$$I_{cb}^2[H^2 - (|\omega_{ze}|\ I_{zz})^2] = (H\Omega_r/\Omega_n)^2 \qquad (7)$$

Equation 7 assumes that the normalised wheel momentum, γ, is approximately equal to Ω_r/Ω_n (rather than H_r/H) which is valid since in normal attidude the body momenta are negligible when compared with the nominal wheel momentum ($I_r\ \Omega_n$), i.e. $H \simeq I_r\Omega_n$. Clearly, if ω_{ze} can be found for two different subcritical wheel speeds Ω_r, then it is straightforward to evaluate I_{yy} and I_{zz} using Eq. 7. The third spacecraft inertia value I_{xx} may be determined from Eq. 8 which gives the nutation frequency ω_n at nominal wheel speed Ω_n.

$$\omega_n^2 \simeq H^2/I_{xx}I_{zz} \qquad (8)$$

3. SIMULATION

A simple model of spacecraft motion based upon the rigid body dynamic equations of angular momentum (Eqs. 1-3) has been used in the study to assist in the preliminary evaluation of the spacecraft spin behaviour and eventually in the design of the H_{xs} control loop. For the model to be simulated on a desktop computer, typically an IBM PC, the sequence of simple discrete momentum equations specified in Eqs. 9-12 are used.

$$(H_r)_{N+1} = (H_r)_N + T \cdot t \qquad (9)$$

$$(H_y)_N = (H_{ys}+H_r)_{N+1} = [H^2-(H_{xs})_N^2 - (H_{zs})_N^2]^{\frac{1}{2}} \qquad (10)$$

$$(H_{xs})_{N+1} = (H_{xs})_N + [(H_y)_{N+1}(H_{zs})_N/I_{zz} - (H_{zs})_N\,(H_{ys})_{N+1}/I_{yy}] \cdot t \qquad (11)$$

$$(H_{zs})_{N+1} = (H_{zs})_N + [(H_{xs})_{N+1}(H_{ys})_{N+1}/I_{yy}$$

$$- (H_y)_{N+1}\,[(H_{xs})_{N+1} + (H_r)_{N+1}/P]/I_{xx}].t \quad (12)$$

The integration time step is t and a 'perturbation' term characterised by the constant P (Eq. 12) is included to facilitate matching between simulated and actual spacecraft spin behaviour. P must be estimated for a real spacecraft along with the inertias.

An alternative version of the spacecraft model was also programmed to simulate the spin dynamics in the presence of energy dissipation. Energy dissipators are modelled as damper wheels aligned with each of the three spacecraft axes, producing damping torques which are proportional to the relative motion between the wheels and spacecraft body. Using this latter model, Fig. 5 shows how a momentum biased spacecraft 'tumbles' from its original nominal configuration represented by small nutation at the centre of the momentum axes, when the momentum wheel is allowed to run down to a constant subcritical speed. Initially the spacecraft core energy is relatively high, resulting in large precession about one of the $H\sin\theta_z$ stable points on the H_{zs} axes. However, in the presence of energy dissipation due to damper wheels with arbitrarily large damping inertias, the projected H quickly settles down to the stable equilibrium point. Similar behaviour is also simulated when the momentum wheel is run up to its nominal value, except the stable point of interest is moved back to the centre of the axes.

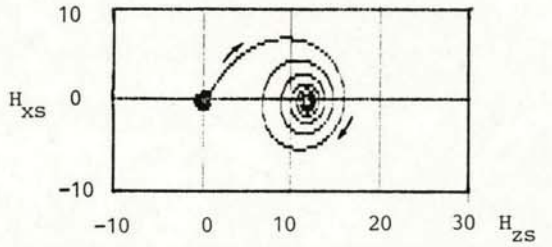

Fig. 5 Flat spin nutation damping by energy dissipation

Such spacecraft spin behaviour has been thoroughly analysed in Ref. 1. There it is demonstrated that specially designed mechanical energy dissipating mechanisms on-board a momentum biased spacecraft can be used for the recovery of nominal attitude from an arbitrary tumbling state. However, within this study an active rather than a passive means, i.e. the H_{xs} control loop is proposed to minimise spacecraft core energy. Any additional energy dissipating mechanism such as fuel slosh which may be present on-board the spacecraft are regarded as an assisting factor, improving the overall recovery performance. As such, no effort has been expended to model these mechanisms in assessments by simulation of the control loop performance.

Fig. 6 (a) shows the initial large spacecraft nutation caused by a fairly fast despin of the momentum wheel to a constant subcritical speed resulting in most the H_r momentum being transferred to H_{ys}. Tne H_{xs} control loop is then applied. In order to demonstrate the effectiveness of the algorithm in minimising spacecraft core energy about a fixed wheel speed, the control wheel torque settings (refer Fig. 4)

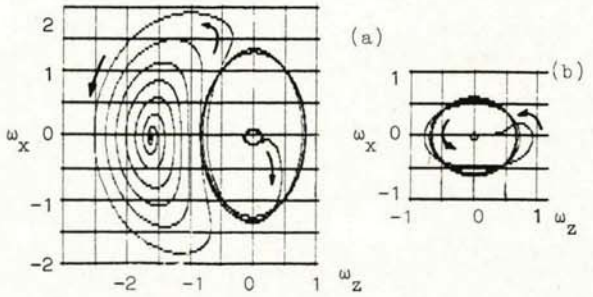

Fig. 6 Simulated pitch nutation damping by H_{xs} loop

chosen are $T^0 = 0$, $T^+ = 0.002$ Nm and $T^- = -0.002$ Nm. The result clearly shows the convergence of the spin dynamics towards the expected stable point on the H_{zs} axis.

The same control in the corollary example in Fig. 6(b) shows the convergence to the stable point at the centre of the momentum axes. The initial nutation in this case is with the wheel at above critical wheel speed as, for example, from an attempt to recover from a large nutation or flat spin condition by spinning up the momentum wheel quickly in an uncontrolled fashion. This latter example clearly suggests a plausible strategy for recovery from large nutations at subcritical wheel speeds. A third example is shown in Fig. 7(a): if the momentum wheel is allowed to spin down at a fairly slow rate, e.g. under friction, and the effective 'perturbation' parameter P (Eq. 12) is small, then the spacecraft would 'tumble' and the projected H precess about the equilibrium points on the H_{zs} (or equivalently yaw rate ω_z) axis. The final damping of the precession onto the equilibrium point shown is effected by switching on the H_{xs} control loop at X. Fig. 7(b) demonstrates the recovery from a 'flat spin' configuration. The series of large precessions about stable points on the ω_z axis are due to the spinning up of the momentum wheel at a constant rate. At point Y, the H_{xs} control loop is applied. The spin dynamics converge to the stable points on the ω_z axis before finally settling down to small nutation about the nominal stable orientation at wheel speeds above the critical value. It should be emphasised that the target is for the projected H to be very close to its final stable orientation as the wheel speed reaches the critical value. Then, a reasonably large wheel torque would be applied in order to minimise the final nutation.

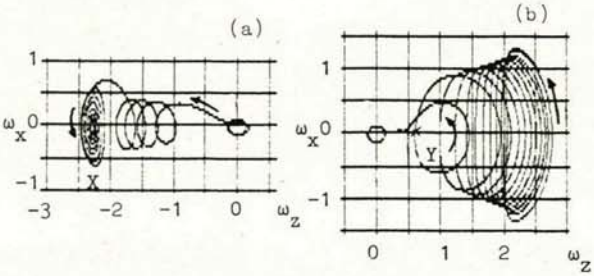

Fig. 7 (a) Simulated nutation damping at X;
(b) Recovery by wheel spin up followed by applying H_{xs} loop at Y

The above examples assumd a processing delay of 30 seconds between the computation of wheel torque demand T and its implementation, in conjunction with a first order predictor for H_{xs}.

The final example in Fig. 8 illustrates the application flexibility of the H_{xs} control loop. By setting a negative T^0 value (Fig. 4) to reduce the wheel momentum, the H_{xs} control loop may even be used to put the momentum biased spacecraft into the final stable flat spin configuration (H_{zs} = H) in a controlled manner. One potential application for this exercise might perhaps lie in the concept of putting in-orbit spare spacecraft into some form of 'hibernation' model.

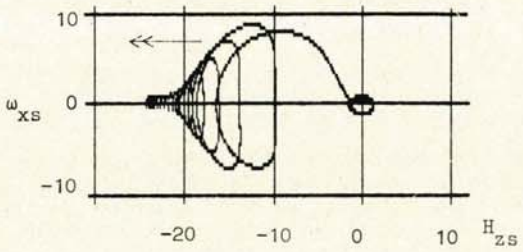

Fig. 8 Simulated flat spin manoeuvre

4. EXPERIMENT

Whilst the technique proposed is suitable for automatic on-board implementation where the delay between data sampling and wheel control demand implementation can be minimised, it has been shown in the analysis to be capable of coping with long TT&C delays which are inevitable with ground implementation. An experiment was recently performed jointly by BAe and ESTEC on OTS to explore the possibility of implementing this fast recovery technique under ground control.

The sequence of events in the experiment was as follows:

(a) With the spacecraft in nominal attitude note the wheel speed and nutation frequency.

(b) Perform a controlled wheel despin to cause the spacecraft to enter a large nutation flat spin.

(c) In the region just below the critical wheel speed (~ within 700 rpm) establish a pitch bias to wheel torque mapping (it is not possible to command wheel torque directly on OTS).

(d) Locate stable equilibrium points on the yaw rate axis for two subcritical wheel speeds.

(e) Using (a) and (d) with Eqs. 7-8, estimate the values of the inertias for the spacecraft model.

(f) Load the spacecraft model into the desktop computer and compare the model with the dynamics observed in (b) to estimate P.

(g) Select T^+, T^0, T^- from (c) and estimate ground processing and implementation delays.

(h) Optimise the control law parameters m, K using the spacecraft model.

(i) Perform a flat spin recovery using the control law.

(j) Recover Earth pointing attitude by a simple pitch slew.

Fig. 9, locus (A) shows the projected H path during event (b), when the despin rate was in the range of 30-39 rpm/min.

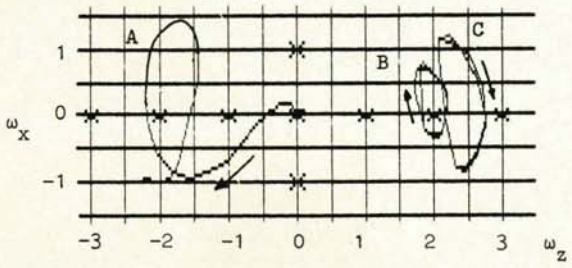

Fig. 9 (A) Wheel despin leading to nutation flat spin;
(B) & (C) Equilibrium point nutations

Fig. 9, loci (B) and (C) illustrate event (d) with stable nutation about equilibrium points $|\omega_{ze}|$ = 2.04 & 2.45 deg/s for average wheel speeds Ω_r = 2161 and 1903 rpm respectively. With these equilibria, knowing Ω_n = 4158 rpm (corresponding to total momentum $H \simeq I_r \Omega_n$ = 25.40 Nms), and ω_n = 0.06584 r/s, Eqs. 4-5 gave (I_{xx}, I_{yy}, I_{zz}) = (357.9, 149.5, 415.7) Kgm². With these inertias applied to the simulation model described by Eqs. 9-12, the 'perturbation' parameter P, was estimated to have an effective value of 90. In event (h), optimization of H_{xs} control law parameters m, K assumed wheel control torque levels $|T^0|$ = 0.003149, $|T^+|$ = 0.009145, $|T^-|$ = 0.006282 Nm and delays of 25.6 s between the sampling and arrival of the relevant telemetry data for the control loop, plus 9.6s between computation and implementation of control wheel torque demand. The results of a quick on-the-spot optimization based on the simulated damping effectiveness of the H_{xs} loop yielded m = 0.05 deg/s and K = 200s.

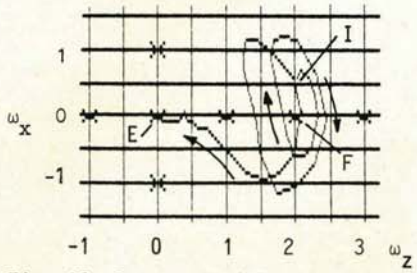

Fig. 10 Recovery with mismatched delay between (I) & (F)

An example in Fig. 10 shows the case of a fast recovery initiated at Ω_r = 2083 rpm (indicated I), when the spacecraft was nutating with an angle of around 40 deg and the pitch body rate was about -2.5 deg/s . The momentum wheel was spin up using control torque demand generated by the H_{xs} loop.

For Ω_r up to 2383 rpm, the T (or corresponding pitch bias) values were telecommanded with a consistent one iteration step delay ($\sim$ 35.2s), resulting in the expected initial divergence of the projected H path. However, from Ω_r = 2383 rpm onwards (at point F) this telecommand delay was reduced to around 9.6s, i.e. the correct value for which the H_{xs} loop was optimised. Fig. 10 shows the resulting recovery from point (F) in the final phase. The flat spin recovery was terminated at (E) when the yaw and roll rates had been reduced to 0.085 and 0.08 deg/s respectively at Ω_r = 2750 rpm.

Then a large pitch bias was telecommanded which spun up the momentum wheel with a torque of about 0.045 Nm. The recovery time from point (I) to (E) was just under 20 minutes. A corresponding simulated recovery based on a matched telecommand delay of 9.6s throughout the recovery (i.e. from (I) to (E) is shown in Fig. 11. The control of the projected H path is much tighter, at the expense of slightly longer recovery time of around 35 minutes. A more complex recovery scheme involving coarse and fine deadbands in the H_{xs} control loop may be envisaged in general to minimize the total recovery time.

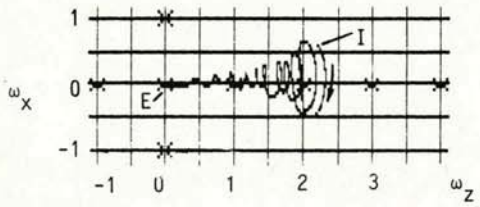

Fig. 11 Simulated recovery with matched delay

The behaviour of the power and thermal subsystems during the recovery experiment were closely monitored. The results verified that in sun-light environment the non-zero pitch rate of the spacecraft throughout the recovery helped to maintain acceptable regular intermittent charging of the battery and the overall thermal balance of the spacecraft. It would be possible to perform the recovery in eclipse provided there is sufficient battery reserve to drive the momentum wheel and the thermal subsystem which are the main loads on OTS.

5. CONCLUSION

A general technique for minimizing the core energy of a momentum biased spacecraft has been presented. The basis of the technique is the reduction of the spacecraft intermediate-inertia axis momentum by the use of a simple control loop with the momentum wheel as the only actuator. A first order predictor may be incorporated into the algorithm in order to extend its effectiveness to applications involving considerable time delays in data acquisition and implementation. This technique may be used for the fast recovery of a momentum biased spacecraft from arbitrary spin configurations including large pitch axis nutation and flat spin. It has also been shown by simulation that the technique can be adapted to perform a controlled manoeuvre to place a possible spare spacecraft from its nominal configuration into a stable 'hibernation' mode in flat spin. It should be emphasised that in both applications the nominal total momentum vector of the spacecraft must be conserved at all times, i.e. no significant external torques or thruster firings are involved, so that the final recovered configuration (out of 'hibernation' in the second application) is the same or at least very close to the nominal.

The effectiveness of the primary application of the technique has been demonstrated both analytically by simulation and experimentally on OTS. The optimal strategy is found to be dependent on the spin configuration at the start of the recovery. For recovery from large pitch axis nutations, if the momentum wheel speed initially is subcritical then the wheel should be spun up to a suitable speed between the critical and nominal values before the control loop is applied with zero nominal wheel torque. For recovery from flat spin configurations, the control loop may be optimised to operate efficiently over a predetermined subcritical wheel speed range close to the critical value. The recovery would then involve spinning up the momentum wheel at an acceptably high rate to minimize recovery time and applying the H_{xs} loop when the wheel speed is within the operating range. These techniques are simple to implement and may be designed to operate on-board the spacecraft for future missions or under ground control in the case of current communications satellites to support fast recoveries from arbitrary spin.

6. REFERENCES

1. Hubert C. 1978, Spacecraft attitude acquisition from an arbitrary spinning or tumbling state, AIAA J. Guidance and Control vol. 4, No. 2, 164-170.

2. Peyrot & Runavot 1978, Study of attitude acquisition system based on momentum exchange, Estec Ref. No. 2842/76/NL/AK/SC.

3. Bird A.G. 1985, Constant phase trajectory for flat spin recovery, an Estec discussion note.